Available online at www.sciencedirect.com
SCIENCE DIRECT
Journal of Non-Crystalline Solids 352 (2006) 2589–2595
JOURNAL OF NON-CRYSTALLINE SOLIDS
www.elsevier.com/locate/jnoncrysol

Characterization of exciton self-trapping in amorphous silica

Renée M. Van Ginhoven [a,1], Hannes Jónsson [b], L. René Corrales [c,*]

[a] Department of Chemistry, University of Washington, Seattle, WA 98195, United States
[b] Faculty of Science VR-II, University of Iceland, 107 Reykjavík, Iceland
[c] Pacific Northwest National Laboratory, P.O. Box 999, MSIN K8-91, Richland, WA 99352, United States

Available online 5 June 2006

Abstract

Triplet electron–hole excitations were introduced into amorphous silica to study self-trapping (localization) and damage formation using density functional theory. Multiple self-trapped exciton (STE) states are found that can be differentiated based on the luminescence energy, the localization and distribution of the excess spin density of the triplet state, and relevant structural data, including the presence or absence of broken bonds. The trapping is shown to be affected by the relaxation response of the silica network, and by comparing results of quartz and amorphous silica systems the effects of the inherent disordered structures on exciton self-trapping are revealed. A key result is that the process of exciton trapping can lead directly to the formation of point defects, without thermal activation. The proposed mechanism includes a non-radiative decay from the excited to the ground state followed by structure relaxation to a defect configuration in the ground state.

PACS: 61.72.Bb; 61.72.Ji

Keywords: Defects; Density functional theory; Silica

1. Introduction

Exposure of silica glass to high energy radiation or particle bombardment is known to cause structural modification. Radiation-induced damage can be observed in materials used in high intensity photon applications, in hostile environments, such as those subjected to radiation in space (satellites, telescopes, laser applications), and in glasses slated for the entombment of nuclear waste materials. Alternatively, it is possible to take advantage of the modifications to tailor structure at the molecular level [1,2]. A better understanding of the factors that control damage processes is needed to design better materials, to predict expected lifetimes, and to learn how to better control fabrication of tailored materials.

Experiments have provided convincing evidence that certain types of damage in amorphous silica involve self-trapped excitons (STEs) [3]. We investigate the process of excitons trapping and the associated structural response in amorphous silica using density functional theory (DFT). The ability of a particular amorphous structure to support different types of excitons, and exciton-induced changes in the amorphous network are examined.

Silica is known to support an STE in the triplet state [4] with an observed luminescence of 2.4 eV [5], similar to that seen in cristobalite at 2.4 eV but lower than that of quartz at 2.8 eV. Luminescence peaks in amorphous materials show significant inhomogeneous broadening due to contributions from many different local geometries. Time-resolved data show that the luminescence energy increases over time, and has non-exponential decay, indicating multiple lifetimes, and possibly a distribution of different states [6]. In about 1% of STE states created, the decay channel back to the electronic ground state leads to a damage state [7]. For such damage mechanisms the experimental

* Corresponding author. Tel.: +1 509 376 6608; fax: +1 509 376 0420.
E-mail addresses: hj@hi.is (H. Jónsson), rene.corrales@pnl.gov (L.R. Corrales).
[1] Sandia National Laboratory, Albuquerque, NM, United States.

0022-3093/$ - see front matter © 2006 Elsevier B.V. All rights reserved.
doi:10.1016/j.jnoncrysol.2006.01.095

evidence indicates that there is rupturing of Si–O bonds, accompanied by the displacement of oxygen atoms [5,8]. Different defects are believed to be formed by the action of a single STE, or by the interaction of multiple STEs [9,10]. Induced defect structures have been identified as likely precursors to the observed interstitial molecular oxygen [11–14].

In this work, excitons in amorphous silica are studied with the same level of DFT as that used previously for quartz [15–17]. Such an approach enables a direct comparison between crystal and amorphous states that reveals the physics imposed by the inherent disorder of a glass. The simulation of amorphous silica presents a significant technical challenge in itself that is exacerbated by the limitation of DFT methods that constrains its use to relatively small system sizes. Recently, the combination of computer power and the development of state of the art methodologies has made it possible to capture characteristics of the glassy medium range order using DFT [18,19], so that it is feasible to perform more sophisticated studies involving complex processes.

2. Theoretical procedure

Calculations and simulations employed gradient corrected DFT as provided by the Vienna ab initio simulation package (VASP) [20,21] with the PW91 functional [22]. Spin-polarized DFT was employed for all triplet state calculations, and for singlet state geometries with broken bonds. The ions were represented by Vanderbilt ultrasoft pseudopotentials [23] using a plane-wave basis set with an energy cutoff of 396 eV, and augmentation charge cutoff of 829 eV. Only the Γ point for the Brillouin-zone integration was used, as that has been shown to be sufficient in earlier work on excitons in quartz [24]. The minimum energy paths described below were calculated using the climbing-image-nudged-elastic-band method (CI-NEB) [25,26].

Two simulated glass samples were selected for this study from several unique amorphous structures of silica generated and structurally characterized in previous work [19]. The glass systems consist of 72 atoms (24 silicon and 48 oxygen atoms) that statistically represent the short- and intermediate-range structure distributions as compared to a large simulated glass structure. The reader is referred to that reference for details on how the structures were obtained, optimized and analyzed. Glass samples with perfect coordination were selected because the presence of a defect site can localize an exciton where it can undergo further transformations and would otherwise interfere with the intentions of this work [27].

The use of small periodic systems with cell sizes of about 10 Å is justified because they are able to capture much of the relevant medium range order of silica glasses that lies in the range of 5–15 Å [28], and self-trapping of excitons is expected to occur within a localized molecular environment, involving no more than a few tens of atoms [29]. It has been shown that structural rearrangements due to chemical reactions are well captured within this range [30].

Optimization of the structures was done using an iterative conjugate-gradient minimization scheme, with a convergence criterion of 0.01 eV $Å^{-1}$ for inter-atomic forces in both the singlet and triplet state. A convergence criteria of 10^{-4} eV was used for the electronic energy at each step in the optimization. For single point calculations, a 30% increase in the number of plane-waves was used to obtain high precision to sufficiently converge the energy with respect to the basis set.

Three simulation methods were employed to discover exciton configurations for each sample. In the first method, the ion positions were allowed to relax at zero temperature on the triplet state surface to find the 'default' exciton. In the second method, the glass samples were heated to 300 K while in the triplet state by running constant energy dynamics, and scaling the velocities every 20 steps for 0.5 ps. The simulation was then continued using the Nosé thermostat for an additional 1.5 ps, followed by a quench to 0 K. Excitons found using this method are referred to as 'thermally induced excitons'. The third method introduces local distortions in the system consisting of displacing either a silicon or oxygen atom between 0.05 and 4 Å. Unique structures found in this manner are called 'displacement induced excitons'. The cell volume, optimized for this level of theory, was held fixed for each simulation.

In the figures that illustrate each exciton, the location is indicated by isosurfaces of the excess spin density. The regions corresponding to the excited electron and the hole are separated by comparing the α and β densities of the triplet state to those of the singlet state for the same ion positions. The excited electron is where the α density is increased relative to the singlet, and the hole is located where the β density is decreased relative to the singlet. The localization of the exciton is quantified by determining the participation ratio of the excess spin density. A population analysis of the spin per each atom was calculated using Bader analysis [31]. The participation ratio was calculated based on the excess n population summed onto the atoms of the system, as in previous work on quartz [17]. P_{spin} will tend to change with the number of atoms in the sample, but since each sample had 72 atoms, this calculation yields a useful measure of the relative localization of the STE. The quantities of interest are the total participation of the spin density and the distribution of the spin density population among the atoms that are part of the STE.

3. Results

Exciton results are summarized in Table 1. The lattice relaxation energy, E_{Relax}, is the difference between the energy of the final optimized triplet state, and the triplet state of the original ground state geometry (initial excitation energy). A negative value for the lattice relaxation energy means that the system ends in a local minimum that is higher in energy than the initial excitation energy, imply-

Table 1
Participation ratio, distribution of excess spin density, selected structural information, and assignment of exciton type for the excited states in amorphous silica and quartz

Sample	T_1–S_0	ρ (g/cc)	State	P_{spin}	Distribution			STE type
					Si/O/O/O	E_{Relax}	E_{Lum}	
G1	5.61	2.26	Default	1.02	4/4/4/3	0.06	5.48	Deloc.
			Therm	1.21	35/20/19/12	0.14	2.36	B
			D1	1.31	38/38/8/6	0.33	0.73	Si-dist
			D2	1.19	33/24/11/8	−0.29	3.25	B
			D3	1.29	35/41/5/5	−0.7	1.20	A
G2	5.56	2.27	Default	1.02	3/3/3/2	0.06	5.39	Deloc.
			Therm	1.28	37/36/11/4	0.95	0.04	A
Quartz	6.1		Default	1.01	2/2/2/2	<0.01	6.0	Deloc.
			Fixed	1.33	27/49/7/3	−0.93	2.74	A
			D1	1.16	31/18/14/12	−0.43	3.72	B
			D2	–	–	−0.65	0.9	Si-dist

P_{spin} is the participation ratio of the excess spin density. The distribution column lists the percentage of spin population associated with the four atoms that have the greatest spin population. The excitons are divided into Deloc. (delocalized), type B, which has a local distortion but no broken bonds, and type A which have broken bonds. T_1–S_0 is the initial singlet–triplet splitting at the optimized singlet state geometry. E_{Relax} is the network relaxation energy, and E_{Lum} is the luminescence energy, as defined in the text. All energies are reported in eV.

ing the existence of a barrier on the triplet state surface between this state and the initial excitation such that the self-trapped state is metastable relative to the delocalized state. The luminescence energy, E_{Lum}, is the difference between the triplet and singlet state energy evaluated at the geometry optimized for the triplet state. When E_{Lum} is small (smaller than around 1 eV), the transition back to the singlet ground state is expected to be a non-radiative transition.

The default exciton for both glasses occurs as a delocalized state with no sign of self-trapping. These delocalized excitons involve little lattice relaxation in terms of both energy and total distance moved by the ions where the relaxation is spread over a large part of the lattice, and the luminescence energy is close to the initial singlet/triplet splitting. The excess spin density is delocalized over ten or more oxygen atoms in the network. The structure and excess spin density for the delocalized excitons are shown in Fig. 1.

Thermal annealing led to distinct localized exciton states for both glasses lower in energy than the default delocalized state, as indicated by the network relaxation energy shown in Table 1. The thermally induced excitons fall into two categories, labeled type A that has a broken Si–O bond, and type B that has a local distortion in the network in which all of the Si–O bonds on one silicon atom are stretched. The B and A labels correspond to the labels assigned previously to similar STE types in quartz [17] where corresponding structure response is described further below.

The structure and excess spin density of the thermally induced exciton in glass G1 is shown in Fig. 2(a). The spin density is localized on one silica tetrahedron where the excited electron is on the silicon atom, and the hole is

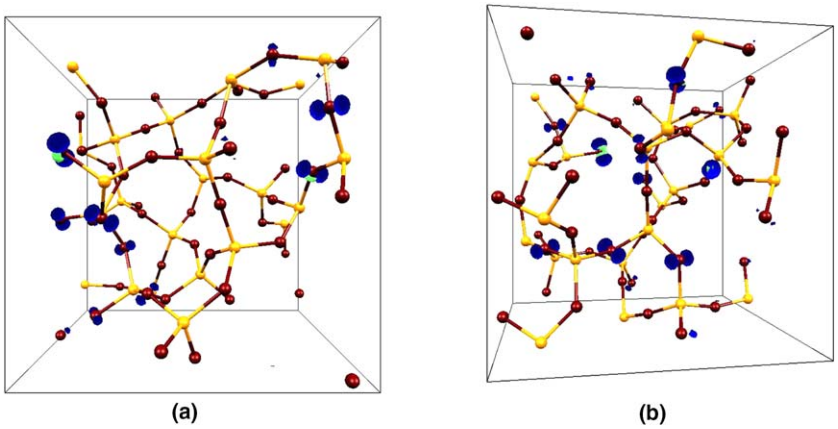

Fig. 1. The structures of the default excitons for glasses G1 and G2. The yellow spheres represent silicon atoms, and oxygen atoms are red. The green cloud indicates an isosurface of the excess spin density corresponding to the excited electron, and the dark blue cloud indicates the location of the hole. An isosurface of 0.1 $e^-/Å^3$ was used. These excitons are delocalized over several oxygen atoms in the configurations.

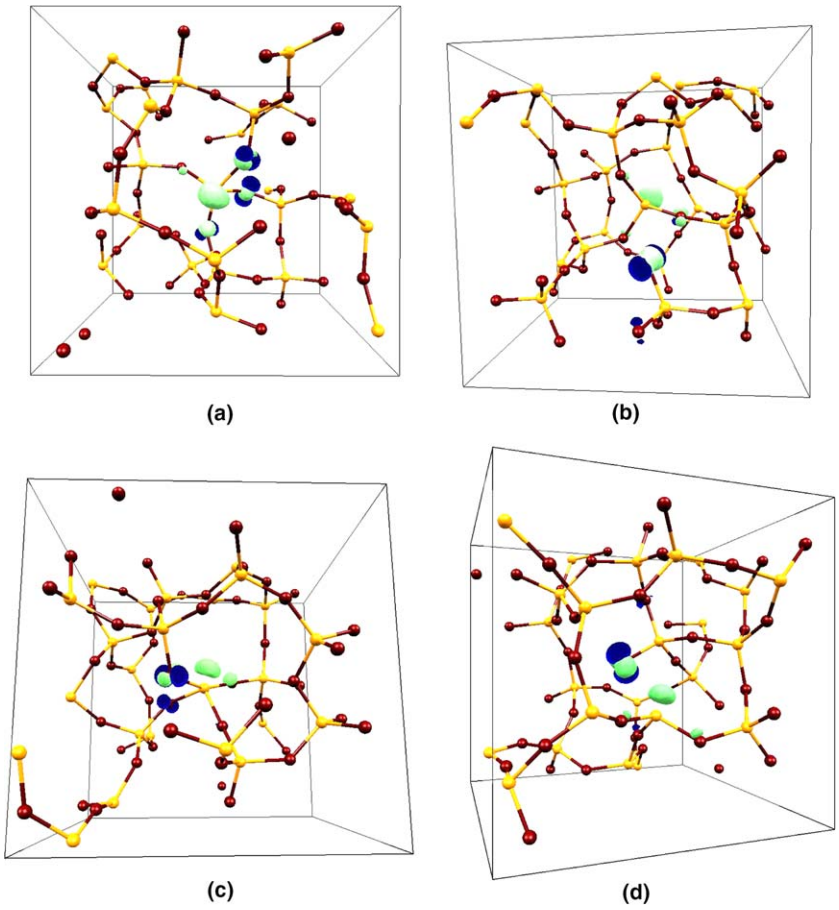

Fig. 2. The structure of the localized excitons for glass G1. The color scheme is the same as in Fig. 1. The spin density isosurface is set to 0.425 $e^-/Å^3$. (The 0.425 $e^-/Å^3$ isosurface is not visible for the delocalized excitons.) Each exciton is localized on one silicon atom and the neighboring oxygen atoms. The labels are consistent with Table 1. (a) The thermally induced exciton. The Si–O bond distances at the STE site are stretched to 1.74 Å, 1.81 Å, 1.77 Å, and 1.71 Å. (b) STE D1. The silicon atom at the center of the figure is puckered back through the plane of the three attached oxygen atoms. The distance between the silicon atom and the oxygen atom in the foreground is 3.04 Å. (c) STE D2. The Si–O bonds are stretched to 1.88 Å, 1.72 Å, 1.71 Å, and 1.67 Å. One O–Si–O angle is flattened to 161°. (d) STE D3. The distance across the broken bond is 2.72 Å.

shared primarily over 3 of the oxygen atoms. The thermally induced localized exciton for glass G2 is shown in Fig. 3(a) and (b). An Si–O bond is broken, and the Si–O distance increases significantly. The electron is located on the silicon atom, and the hole is located on the dangling oxygen atom, with some sharing with a nearby network oxygen atom. This STE leads to an alteration of the network structure when de-excited and relaxed in the singlet state, as discussed further below.

Additional distinct STE states were obtained for glass G1 by inducing displacements at different atoms throughout the structure. The displacement-induced excitons, D1–D3 are shown in Fig. 2(b)–(d), and results are listed in Table 1. State D1 has a structure type consisting of a broken bond and a 3-fold coordinate silicon atom displaced back through the plane of the remaining 3 oxygen atoms. The electron is located on the silicon atom, and the hole is located on the dangling oxygen atom. Both the optimized geometry, and the calculated luminescence energy of 0.73 eV, are similar to a state found in quartz, referred to as the Si-dist state [24]. D2 and D3 have structure types STE-B and STE-A, respectively, as in the thermal excitons. Specifically, D2 is of type STE-B where the excited electron is localized on one silicon atom, and the hole is shared amongst three of the oxygen atoms. No bonds are formally broken, but all four Si–O bonds were stretched. The luminescence is 3.25 eV. Although similar to that found for the thermally induced STE in glass G1, it occurs in a different region of the sample. D3 is of type STE-A where the excited electron is on the silicon atom, and the hole is on the dangling oxygen atom.

In glass G2, an STE-activated damage process was found. The excited state first relaxes towards localization, and because the singlet and triplet state surfaces are nearly degenerate near the STE state, the de-excitation is non-radiative. Once returned to the ground state, the system evolves along the singlet state surface to a new higher-energy configuration. Fig. 3 shows the evolution of the structure from the starting (defect-free) singlet state, to the optimized STE state, to the new rearranged singlet state structure resulting in a 5-fold coordinated silicon atom, and a 3-fold coordinated oxygen. This defective structure

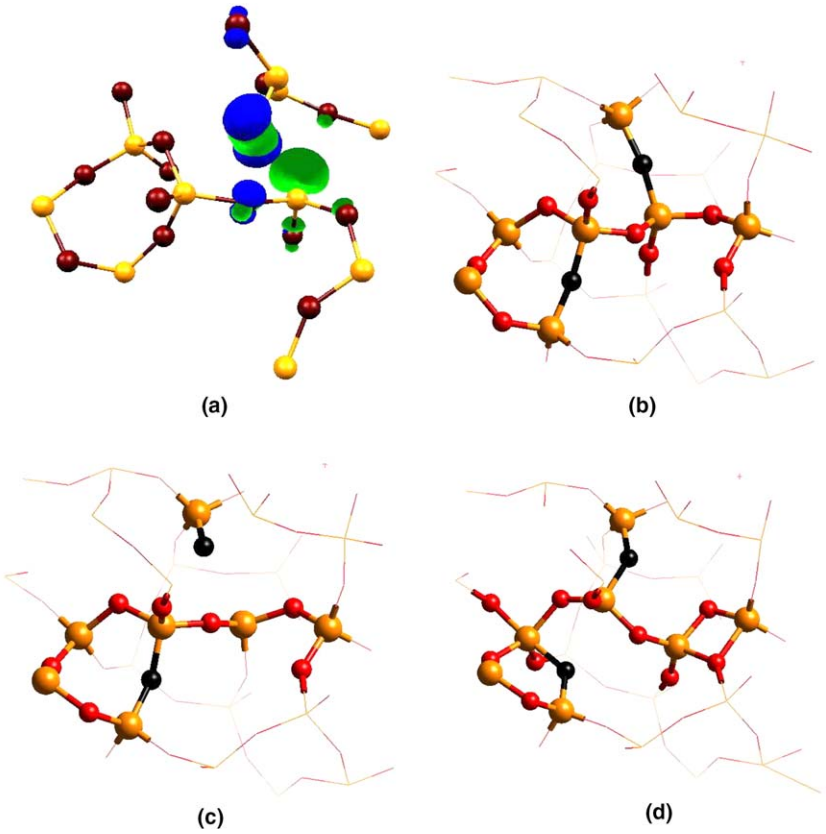

Fig. 3. (a) The structure of the thermally induced exciton for glass G2. The color scheme and isosurface are the same as in Fig. 2. The exciton is localized at a broken bond, with an Si–O distance of 3.21 Å. The distance between the dangling oxygen atom and the nearby oxygen atom that shares the hole is 2.33 Å. (b)–(d) Structural rearrangement seen in glass G2 as a result of the action of the thermally induced exciton. (b) The initial optimized singlet state structure. (c) The thermally annealed triplet state STE structure. One Si–O bond is broken. After de-excitation back to the singlet state, atoms move to form the metastable structure seen in (d). The oxygen atoms that are bonded to different silicon atoms than in the defect-free glass are shown in black. The cut-out region shows that the new structure has a 5-fold silicon, 3-ring (on the left), and a 3-fold oxygen and edge-sharing tetrahedra (on the right). The over-coordinated silicon and oxygen atoms are 6.3 Å apart. This structure is 1.2 eV higher in energy than the defect-free structure.

may be thought of as a type of Frenkel pair defect. It is 1.2 eV higher in energy than the defect-free ground state. Fig. 4 shows the triplet and singlet state energy curves for the structural evolution of the system. The barrier back to the defect-free ground state on the singlet state surface, shown in the inset of Fig. 4, is 0.76 eV. The MEP is not simply the reverse of the formation process (this has a barrier of 3.4 eV), but instead involves a concerted motion of 5–10 atoms so as to avoid creating any broken Si–O bonds on the way back to the original 'healed' configuration.

4. Discussion

The behavior of amorphous silica in the presence of a triplet exciton was studied, and several types of excitons were found, with varying degrees of localization. Delocalized excitons and localized STEs can be differentiated unambiguously based on the P_{spin}. For the delocalized excitons P_{spin} is close to 1.0, whereas all the localized STEs have P_{spin} greater than 1.1. It is possible to further distinguish between type B STEs, which have a local distortion but no broken bonds, and A type STEs which have a broken bond, on the basis of P_{spin}. The type B STEs are clearly less localized because they have P_{spin} of 1.16 to 1.20. In contrast the type A STEs have P_{spin} between 1.27 and 1.34. In addition, type B STEs tend to have higher luminescence energy.

The results for amorphous silica can be compared directly to previous results for quartz. When the same level of theory is used, both quartz and an idealized amorphous structure support the same four basic types of excitons initially found in quartz, namely, the delocalized state, the A, and B STEs, and the Si-dist state. Recent work by others at a different level of theory [32] correctly eliminates the artificially low energy delocalized exciton, but does not indicate the possibility of the formation of other STE types. It must be noted that the reduced size of their quartz crystal supercell significantly reduces the possible network response. Calculations currently underway using an alternative higher level of theory based on exact exchange predict multiple STE states [33].

Differences between amorphous and crystal silica include that the delocalized excitons in the amorphous samples are slightly more localized than the delocalized state in quartz, with $P_{spin} = 1.02$, as compared to 1.01 in quartz. The increased localization for the amorphous

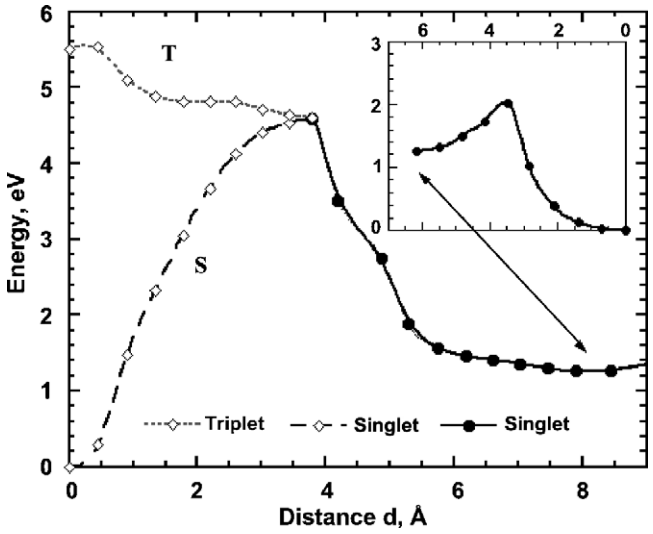

Fig. 4. The triplet and singlet state energy curves along a path for an exciton driven network rearrangement event in glass G2. At the far left, $d = 0$, is the default triplet state minimum obtained by minimization on the triplet state surface after direct excitation from the singlet state. After thermal annealing for 1 ps at $T = 300$ K in the triplet state, a lower energy structure was found ($d = 3.8$). The minimum energy path between the two is shown by a dotted line labeled T. The singlet state energy for the same configurations is shown as a dashed line labeled S. After de-excitation back to the singlet state, the system evolves further and there is rearrangement of the network in which 5 atoms change their bonding and/or coordination state ($d = 8$). The inset shows the barrier for the singlet state path back to the original state from the defect state.

samples is expected, due to the inherent disorder present in amorphous systems. The reduction of the extent of delocalization is expected no matter what level of theory is used. Clearly shown in this work is that unlike in quartz, some localized STE states are lower in energy than the delocalized state. This result is due to the inherent disorder, and greater network response of the amorphous structure. Localization of the exciton at a single tetrahedron allows the bonds at that site to stretch or break, enabling relaxation and release of strain in the surrounding network, which results in an energy gain sufficient to offset the artificial lowering of the energy of the delocalized exciton. Some STEs were found that are higher in energy than the delocalized state. Their relative energy may be partially attributed to the theoretical methods used in this study, but it is also possible that states inherently metastable with respect to the delocalized state occur in glassy silica. More work is needed to determine the role of metastable STEs in exciton migration across a glass. Future work using exact exchange within DFT is currently under way that will further reveal the role and existence of multiple STE types.

Central to this work is the discovery of a damage process pathway that is activated by the exciton self-trapping process. Relaxation of the system on the triplet state surface moves the system to a geometry that is in a new potential energy well on the singlet state surface. Subsequent return to the singlet state surface allows the system to progress into a damage state. In this case, the singlet and triplet state surfaces are nearly degenerate near the STE geometry, so the transition is essentially non-radiative, and the triplet state short-lived. The damage mechanism reported here is the first such mechanism proposed where the glass structure contains no pre-identified reactive site, such as a highly strained bond or edge-sharing tetrahedra [34]. Note that while a glass sample can show STE-induced damage, no damage processes were seen in quartz. While exact exchange is expected to play an important role in the luminescence energy, related to the band gap energy, thus far, little effect is seen in the structural response and the damage path discovered here has not been altered [33].

5. Conclusion

We have shown that the trapping process of an exciton in amorphous silica can lead directly to network modification or damage, in this case via a non-radiative decay channel. We also show that the disorder present in a glassy system facilitates exciton trapping because there is energy gain from the network relaxation. As a result, localized STEs can be lower in energy than the delocalized state. This is in contrast to results for quartz, where the delocalized exciton is the lowest energy state due to the limitations of the DFT method. Finally, several self-trapped exciton types were found in amorphous silica that were previously predicted to occur in quartz with this level of theory, where some STE states are at higher energy than the delocalized state. These metastable states should not be confused with the characteristic states found in quartz and could participate in the diffusion of an STE.

Acknowledgments

This work was supported by the Office of Basic Energy Science, Department of Energy. The research was carried out at the University of Washington and at the William R. Wiley Environmental Molecular Sciences Laboratory, a national scientific user facility sponsored by the Department of Energy, Office of Biological and Environmental Research located at Pacific Northwest National Laboratory. Battelle operates the Pacific Northwest National Laboratory for the Department of Energy.

References

[1] J. Chan, T. Huser, S. Risbud, D.M. Krol, Opt. Lett. 26 (2001) 1726.
[2] W. Reichman, J. Chan, D.M. Krol, J. Phys.: Condens. Matter 15 (2003) S2447.
[3] T.E. Tsai, D.L. Griscom, Phys. Rev. Lett. 67 (1991) 2517.
[4] W. Hayes, M.J. Kane, O. Salminen, R.L. Wood, S.P. Doherty, J. Phys. C: Solid State Phys. 17 (1984) 2943.
[5] K. Tanimura, C. Itoh, N. Itoh, J. Phys. C: Solid State Phys. 21 (1988) 1869.
[6] C. Itoh, K. Tanimura, N. Itoh, J. Phys. C: Solid State Phys. 21 (1988) 4693.
[7] D.L. Griscom, in: Proceedings of the Thirty-Third Frequency Control Symposium, Electronic Industries Association, Washington DC, 1979, p. 98.

[8] C. Itoh, T. Suzuki, N. Itoh, Phys. Rev. B 41 (1990) 3794.
[9] T.E. Tsai, D.L. Griscom, J. Non-Cryst. Solids 131–133 (1991) 1240.
[10] N. Matsunami, H. Hosono, Phys. Rev. B 60 (1999) 10616.
[11] H. Hosono, H. Kawazoe, N. Matsunami, Phys. Rev. Lett. 80 (1998) 317.
[12] A.L. Shluger, J.L. Gavartin, M.A. Szymanski, A.M. Stoneham, Nucl. Instrum. Methods Phys. Res., Sect. B 166&167 (2000) 1.
[13] L. Skuja, in: G. Pacchioni, L. Skuja, D.L. Griscom (Eds.), Defects in SiO_2 and Related Dielectrics: Science and Technology, Kluwer Academic, Dordrecht, Netherlands, 2000, p. 73, and references therein.
[14] M.A. Stevens-Kalceff, Phys. Rev. Lett. 84 (2000) 3137.
[15] L.R. Corrales, J. Song, R.M. Van Ginhoven, H. Jónsson, in: G. Pacchioni, L. Skuja, D.L. Griscom (Eds.), Defects in SiO_2 and Related Dielectrics: Science and Technology, Kluwer Academic, Dordrecht, Netherlands, 2000, p. 329, and references therein.
[16] J. Song, R.M. Van Ginhoven, L.R. Corrales, H. Jónsson, Faraday Discuss. (2000) 303.
[17] R.M. Van Ginhoven, H. Jónsson, K. Peterson, M. Dupuis, L.R. Corrales, J. Chem. Phys. 118 (2003) 6582.
[18] J. Sarnthein, A. Pasquarello, R. Car, Phys. Rev. Lett. 74 (1995) 4682.
[19] R.M. Van Ginhoven, H. Jónsson, L.R. Corrales, Phys. Rev. B (2005) 024208, The glass samples G1 and G2 used in this work are the structures labeled Glass 4 and 9, respectively.
[20] G. Kresse, J. Furthmuller, Phys. Rev. B 54 (1996) 11169.
[21] G. Kresse, J. Hafner, Phys. Rev. B 47 (1993) 558.
[22] J.P. Perdew, J.A. Chevary, S.H. Vosko, K.A. Jackson, M.R. Pederson, D.J. Singh, C. Fiolhais, Phys. Rev. B 46 (1992) 6671.
[23] D. Vanderbilt, Phys. Rev. B 41 (1990) 7892.
[24] J. Song, H. Jónsson, L.R. Corrales, Nucl. Instrum. Methods Phys. Res., Sect. B 166&167 (2000) 451.
[25] G. Mills, H. Jónsson, G. Schenter, Surf. Sci. 324 (1995) 305.
[26] G. Henkelman, B. Uberuaga, H. Jónsson, J. Chem. Phys. 113 (2000) 9978.
[27] A.N. Trukhin, J. Non-Cryst. Solids 149 (1992) 32.
[28] R.H. Doremus, Glass Science, John Wiley, New York, 1994.
[29] K.S. Song, R.T. Williams, Self-Trapped Excitons, Springer Series in Solid-State Sciences, vol. 105, Springer, New York, 1996.
[30] R.M. Van Ginhoven, B. Park, L.R. Corrales, H. Jónsson, J. Phys. Chem. B 109 (2005) 10936.
[31] R.F.W. Bader, Atoms in Molecules – A Quantum Theory, Oxford University, Oxford, 1990;
G. Henkelman, A. Arnaldsson, H. Jónsson, Comp. Mat. Sci. 36 (2006) 354.
[32] S. Ismail-Beigi, S.G. Louie, Phys. Rev. Lett. 95 (2005) 156401.
[33] Private communication with H. Jonsson.
[34] T. Uchino, M. Takahashi, T. Yoko, Phys. Rev. Lett. 86 (2001) 4560.